

Development of the Strain-to-Fracture Test

A new test has been established for evaluating ductility dip cracking susceptibility in austenitic alloys

BY N. E. NISSLEY AND J. C. LIPPOLD

ABSTRACT. The strain-to-fracture (STF) test has been developed to determine susceptibility to ductility dip cracking (DDC) and other elevated-temperature cracking phenomena. Samples are tested over a range of temperature and strains, producing temperature-strain cracking envelopes. Threshold strain for fracture (ϵ_{\min}) and the ductility dip temperature range (DTR) can then be extracted from these envelopes and used to compare susceptibility among materials. The test is robust and allows for changes in the testing parameters and material condition to develop a fundamental understanding of factors that affect cracking. Three austenitic base metals were studied: Type 310 stainless steel, Ni-based Alloy 690, and super-austenitic Alloy AL-6XN. Autogenous spot and transverse welds in the three austenitic alloys were tested on-heating using the strain-to-fracture test. Alloy 690 was found to be the most susceptible to DDC with a low threshold strain to fracture and wide DTR. Type 310 stainless steel exhibited a similar DTR to Alloy 690 but had a higher threshold strain. Alloy AL-6XN was found to have the greatest resistance to DDC with a narrow DTR, although the threshold strain over a narrow temperature range was comparable to Alloy 690.

Metallographic examination revealed that intergranular cracking occurred preferentially along migrated grain boundaries (MGBs) in the fusion zone. Cracking was most severe in materials that were free of second phases or precipitates and accordingly had large grain size and straight MGBs. Recrystallization was observed at temperatures near the upper end of the DTR and was accompanied by a recovery of ductility.

Introduction

Ductility dip cracking is a solid-state phenomenon that has been reported in a number of engineering materials, including austenitic stainless steels, Ni-based al-

loys, Cu-based alloys, and titanium alloys (Ref. 1). These normally ductile materials can exhibit a loss of ductility over a temperature range below the solidus temperature. Under the proper conditions, solid-state intergranular cracks form within this elevated temperature range. Such behavior has been called ductility dip cracking (DDC) (Ref. 2). The mechanism for DDC is unclear and tests to determine susceptibility to DDC are often inconclusive. The purpose of this investigation was to develop a test technique that could determine susceptibility to weld metal DDC using a thermomechanical simulator. As a result, the STF test (Refs. 3, 4) has been developed to determine susceptibility to DDC and other elevated temperature cracking phenomenon.

Background

Haddrill and Baker (Ref. 5) defined DDC as a loss in ductility, over a temperature range below the solidus, sufficient to produce cracking under the influence of thermal strain caused by welding. Hemsworth et al. (Ref. 2) defined DDC as occurring above $0.5 T_m$ (T_m = melting point in K) but occurring at boundaries that are free from liquid films. A schematic showing normal elevated temperature ductility as well as the ductility dip is shown in Fig. 1. Ductility dip cracking susceptibility in a material has been quantified by the ductility dip temperature range (DTR) and the threshold strain (ϵ_{\min}) for cracking (Ref. 6). The DTR is defined as the temperature range in which ductility dip cracks occur, and ϵ_{\min} , the threshold strain, as the minimum strain required for cracking to occur — Fig. 1. Zhang et al. (Ref. 7) suggested that for a material to be considered resistant to DDC, the DTR should be less than 100°C (180°F) and/or the threshold strain should be greater than 15%.

Most of the materials susceptible to DDC have a face-centered cubic (FCC) and/or austenitic microstructure. They tend to be single phase from room temperature to melting and solidify as FCC (Ref. 8). It occurs in both weld metal and base metal (Ref. 8), although wrought materials have been found to be more resistant to DDC than autogenous weld metal (Ref. 13). Ductility dip cracking occurs preferentially along migrated grain boundaries (MGBs) in the weld metal of single-phase materials — Fig. 2 (Ref. 9).

Previous tests to evaluate DDC have had difficulties with repeatability due to the number of variables that affect cracking (Ref. 10). Several different techniques have been used to test for ductility dip cracking, including laboratory test welds (Ref. 5), elevated-temperature tensile tests (Refs. 1, 7, 11), the transverse-varestraint (Ref. 11), the double- and triple-bead vareststraint test (Ref. 12), the spot-on-spot (double-spot) vareststraint test (Ref. 13), and the MISO technique (Ref. 7). All of these tests have advantages and disadvantages, but none has emerged as an ideal test for DDC.

Experimental Approach

Many previous tests that have been used to assess susceptibility to DDC are complicated by the fact that weld solidification and liquation cracking may also occur in the samples. Since the DDC and liquation cracking temperature ranges may be very close, it can be difficult to distinguish the two. In addition, the formation of solidification or liquation cracks may locally alter the stress and strain fields in the microstructure, providing some relief of stresses that promote DDC. For these reasons, a Gleeble®-based testing approach was used that would avoid the complications of other forms of elevated-temperature cracking.

Since microstructure has been found to be such an important factor for cracking (Ref. 13), it was determined that this needed to be part of the foundation of the testing technique. Previous experiments with the double-spot vareststraint test (Refs. 13, 14) showed that performing an initial test-spot on the sample developed a

KEY WORDS

Austenitic Alloys
Ductility Dip Cracking
Strain-to-Fracture Test
Recrystallization
Grain Boundary Migration

N. E. NISSLEY and J. C. LIPPOLD are with the Welding and Joining Metallurgy Group, The Ohio State University, Columbus, Ohio.

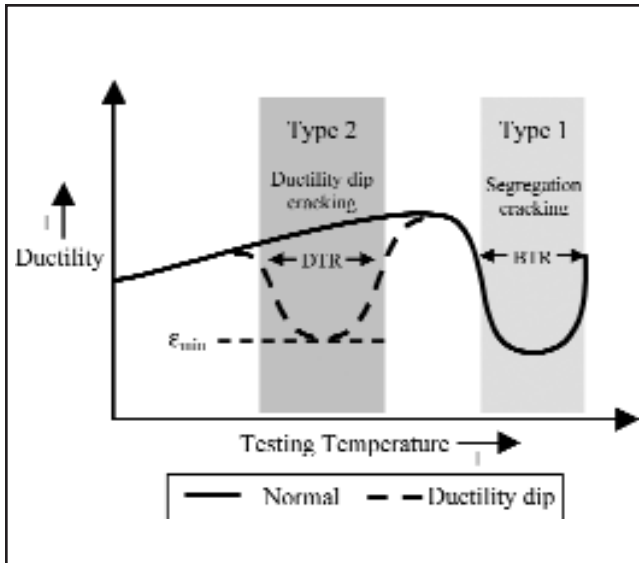


Fig. 1 — Schematic of elevated temperature ductility.

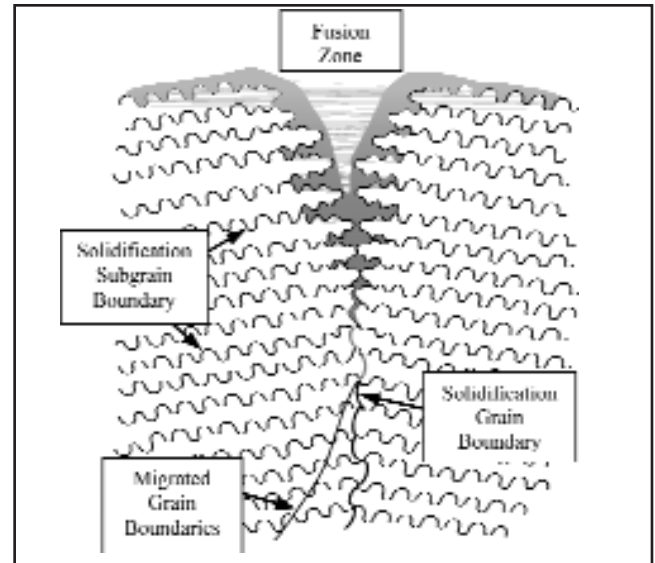


Fig. 2 — Schematic of types of weld metal boundaries observed metallographically in single-phase austenitic weld metals (Ref. 9).

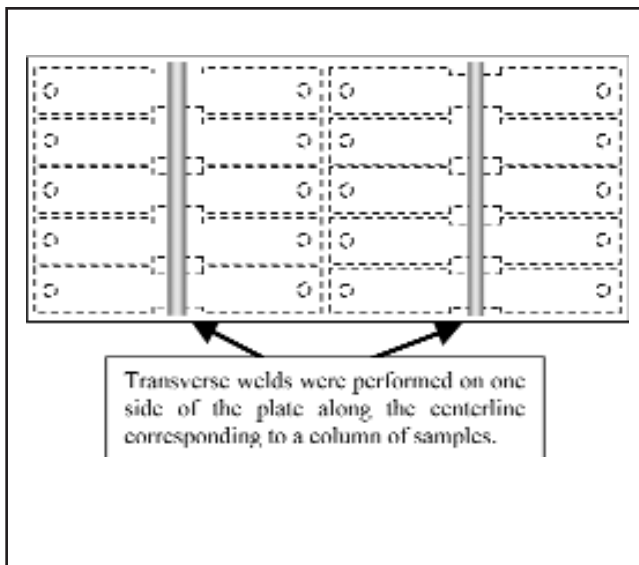


Fig. 3 — Example of sample layout showing location of transverse welds performed on one side of the plate along the centerline corresponding to a column of samples.

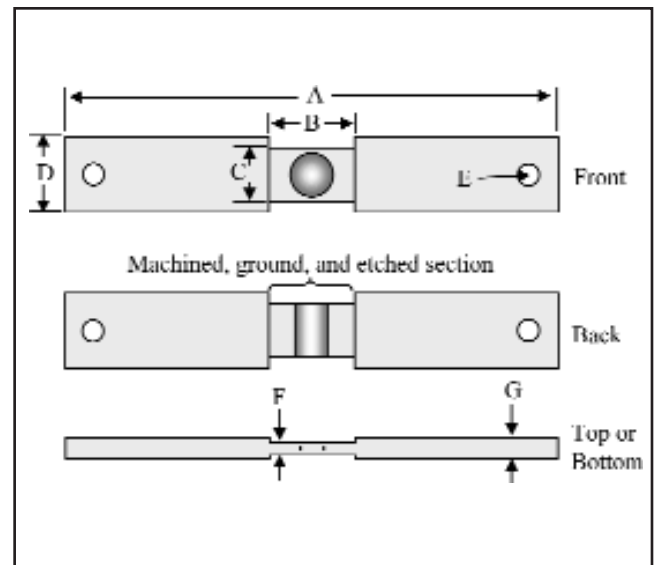


Fig. 4 — Dimensions of final sample: $A = 12.7 \text{ cm}$ (5 in.); $B = 19 \text{ mm}$ ($\frac{3}{4}$ in.); $C = 15.3 \text{ mm}$ (0.6 in.); $D = 19 \text{ mm}$ ($\frac{3}{4}$ in.); $E = 8.3 \text{ mm } \varnothing$ (0.325 in.); $F = \text{ nominally } 5.6 \text{ mm}$ (0.22 in.), (ground until surface is smooth and flat — approximately 0.038 mm [0.015 in.] removed from each side); $G = 6.4 \text{ mm}$ ($\frac{1}{4}$ in.).

favorably oriented microstructure and facilitated consistent formation of DDC. This initial weld (preweld) in the double-spot vareststraint test was determined to be one of the most important parts of the sample design to produce consistent results and was incorporated into the STF test described here.

Experimental Procedures

Materials. The three base materials evaluated for this study were Type 310 stainless steel, Alloy 690, and super-austenitic stainless steel Alloy AL-6XN. Chemical compositions for these alloys

are shown in Table 1. All the materials tested in the study were in the form of hot rolled plate, nominally 6.4 mm ($\frac{1}{4}$ in.) thick.

Sample Preparation. The STF samples consisted of a modified “dog bone” tensile design. Prior to cutting samples from the plate material, continuous autogenous gas tungsten arc (GTA) welds were made at locations coinciding with the reduced section of the STF sample (Fig. 3) with a nominal width of 1.5 cm (0.6 in.). The samples were then cut from the plate using water jet cutting. An autogenous GTA spot weld was then performed within the reduced section on the side opposite the

continuous GTA weld. The diameter of the spot weld was nominally 1.0 cm (0.4 in.), approximately two-thirds the width of the reduced section. Current ramping and weld pool stirring were used during spot welding to control pool shape and solidification conditions. The sample was placed in a copper fixture to prevent reheating of the continuous weld. The GTAW conditions for both spot and continuous welds are listed in Table 2.

Once welding was complete, the sample was machined to the final dimensions shown in Fig. 4. The use of a modified dog bone tensile design helped to concentrate both strain and temperature in the re-

duced section during the test.

Sample numbers and the material types were scribed on the top surface of each sample, away from the center. Gauge marks with a separation of 4 mm (0.157 in.) were made using a Rockwell hardness indenter on both the top and bottom of the samples and recorded to allow for strain measurement following testing — Fig. 4. Prior to testing, the center of the samples were macro-etched using oxalic acid for AL-6XN and Type 310 and chromic acid for Alloy 690, at 2.5 V for 10 to 20 s to show the grain structure and to aid in the evaluation of the regions where cracking occurred. Finally, the samples were screened for discontinuities prior to testing.

Testing Procedure. Samples were tested using the Gleeble thermomechanical simulator. The prepared samples were supported between the jaws of the Gleeble with pins through the holes in the ends of the samples. A jaw spacing of 7.1 cm (2.8 in.) was used. The sample was hydraulically preloaded (manually) to 2200 kg (4850 lb) at room temperature (to prevent sample slippage during testing), and all clamps were adjusted to secure the sample in the jaws before the preload was removed. Testing was performed in a chamber surrounding the jaws evacuated with a roughing pump to 6.7×10^{-3} Pa (5×10^{-5} torr) and then backfilled with 99.95% argon gas. Roughing and backfilling were performed twice to reduce sample contamination. The Gleeble program was then started and the preload was manually applied again to accommodate thermal expansion during heating. The samples were heated to the testing temperature, and the stroke was manually trimmed until the load was approximately zero (to offset thermal expansion). After a set time, the sample was strained to a predetermined distance at the selected test rate. The sample was then held at temperature under the applied strain before it free cooled to room temperature. A schematic of a typical test cycle is shown in Fig. 5. Peak temperature, stroke, and force were recorded with a data acquisition system.

Inspection. After testing, samples were inspected using a binocular microscope at magnifications from 10 \times to 70 \times , although 30 \times was used in most situations. Careful examination was required as light cast on the strained surface would sometimes give the appearance of cracks. Weld bead location relative to the reduced section, number of cracks, and crack location were recorded for reference. The distances between gauge marks were remeasured and the total percent strain calculated.

Optical Metallography. Samples were mounted in plan view to examine cracking apparent on the surfaces of the samples.

Table 1 — Chemical Composition (wt-%) of Study Materials

Element	310 SS	Alloy 690	AL-6XN
C	0.083	0.17	0.021
Fe	Bal.	9.20	46.59
Cr	24.75	26.67	20.95
Ni	18.72	61.06	24.56
Mn	1.42	0.17	0.27
Cu	0.32	0.02	0.23
Si	0.46	0.06	0.48
Al	0.062	0.29	—
Ti	0.014	0.16	—
V	0.054	—	—
Mg	—	0.001	—
Co	—	0.009	0.17
Mo	0.27	0.02	6.32
Nb	—	0.01	—
B	—	0.001	—
N	—	0.009	0.23
O	—	0.004	—
P	0.024	0.004	0.023
S	0.004	0.001	0.0003

Table 2 — Welding Parameters for GTAW Prewelds

Parameter	Time/Setting	Level/Type
Shielding gas preflow	10 s	Argon
Current up-slope time	5 s	~26 A/s
Weld (time is material dependent)	20 – 30 s (for spot only)	130 A
Current down-slope time	12.7 s	~10 A/s
Shielding gas postflow	15 s	Argon
Arc length	2 mm (0.079 in.)	10–12 V
Gas flow rate	20 ft ³ /min	Argon
Travel speed (transverse only)	10 cm/min (0.4 in./min)	—

Table 3 — Initial Conditions Developed to Test Effect of Individual Variables Using Type 310 SS

Variables	Value
Test temperature	1000°C
Heating rate	100°C/s
Stroke rate	0.06 cm/s
Time at temperature	10 s before the stroke, stroke, and 10 s after the stroke
Type of preweld	Spot on one side and transverse on the other
Peak temperature	1000°C (not to exceed the test temperature)
Number of heating cycles	1

The samples were polished through 0.05- μ m alumina and electrolytically etched with either 10% oxalic (Type 310 and AL-6XN) or 10% chromic acid (Alloy 690) at 2.5 V for approximately 5 to 10 s. An effort was made to minimize the material removed as a majority of the cracks were on the surface and relatively shallow. The polished and etched samples were examined using a Nikon metallograph and mi-

crographs were taken using a Hitachi digital camera.

Results

Procedure Development

The initial goal of this research was to develop the test framework and a set of standard conditions for evaluating DDC.

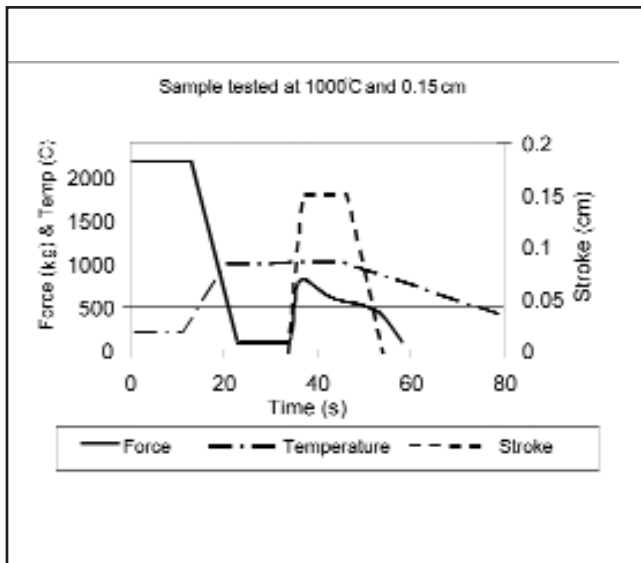


Fig. 5 — Representative test cycle from a STF test.

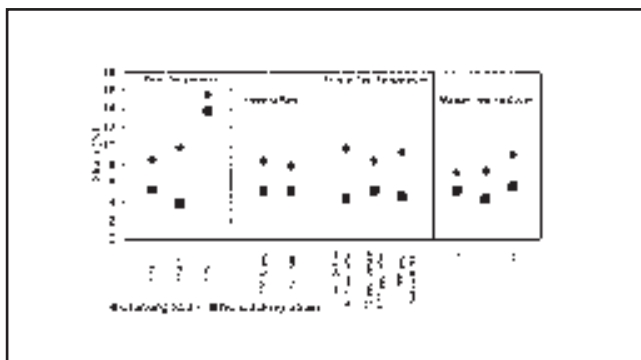


Fig. 7 — Graphical comparison of effects of peak temperature, heating rate, and hold time at test temperature showing common range of STF threshold on Type 310 SS tested at 1000°C.

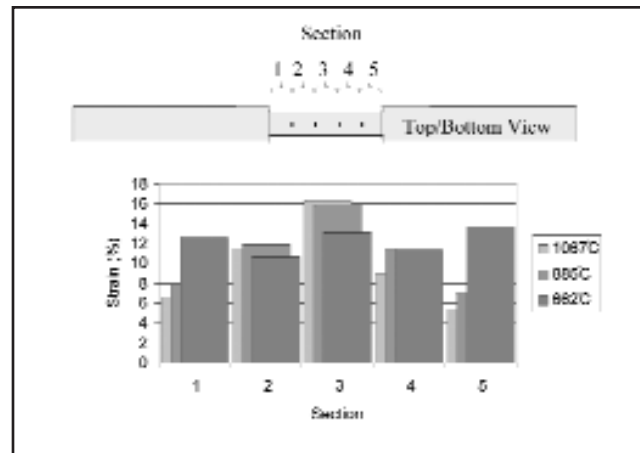


Fig. 6 — Strain variation across the center of samples with peak temperatures of 662, 885, and 1067°C. Section 3 is the 4-mm section used to determine strain in standard testing.

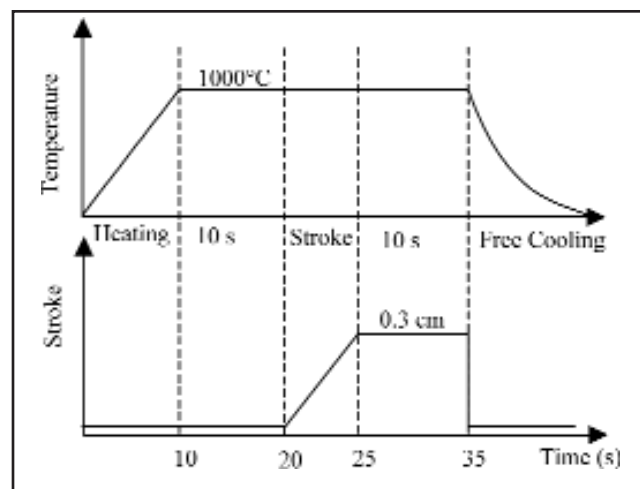


Fig. 8 — Example of 1000°C sample with 10 s before stroke, 10 s after stroke, and a stroke of 0.3 cm at 0.06 cm/s.

For the preliminary testing, Type 310 stainless steel was chosen as the baseline alloy. The Gleeble was chosen as the means of heating and straining the sample because of its control and feedback capabilities. The sample geometry was a modification of the double-spot varestment sample that included the preweld but was modified to fit in the Gleeble. In order to determine the effect that different conditions had on testing, a set of standard conditions was initially established and then each one of the conditions was changed sequentially to determine individual effects. These conditions are listed in Table 3. The effect of each parameter on the minimum strain to fracture (ϵ_{min}) was used to evaluate the effect of each.

Gauge Section Determination. After reviewing the gauge section (distance between gauge marks) parameter, two primary factors are evident. First, the gauge section should be as small as practical to reduce averaging of the strain caused by

the nonuniform thermal distribution across the center of the sample. Secondly, the gauge section should be as large as possible to reduce operator error when measuring strain. To evaluate the strain across the reduced section, punch marks were made every 4 mm, creating five gauge sections — Fig. 6. The strain distribution across the reduced section was then measured for three different temperatures. At lower temperature, the strain was fairly uniform, but at higher temperature, the strain was concentrated in the center of the reduced section. This confirmed that larger gauge sections would produce a strain that was averaged over a larger area. The averaged strains would not represent as accurately the true strain occurring in the center of the sample where the majority of the cracking occurred. In addition to this, cracking normally occurred within the center 4 mm of the specimen in all cases. As a result of these findings, an initial gauge section of 4

mm was chosen as a compromise between these two factors in an attempt to minimize their effects.

Peak Temperature. In order to determine the effect that peak temperature had on DDC, several samples were evaluated at three peak temperatures. All of the samples were heated to a peak temperature, held for 10 s, cooled at 10°C/s (18°F/s) back to 1000°C (1832°F), and then immediately strained. The three peak temperatures that were evaluated were 1000, 1100, and 1250°C. Samples were run at each temperature using different stroke lengths until two samples were obtained that straddled the cracking/no-cracking threshold. Results of tests at the three temperatures are displayed in Fig. 7.

These data suggest that there is an effect of peak temperature on cracking susceptibility. However, it is not clear from the data if the effect is only at 1250°C or if it is also at 1100°C. Heating to higher tem-

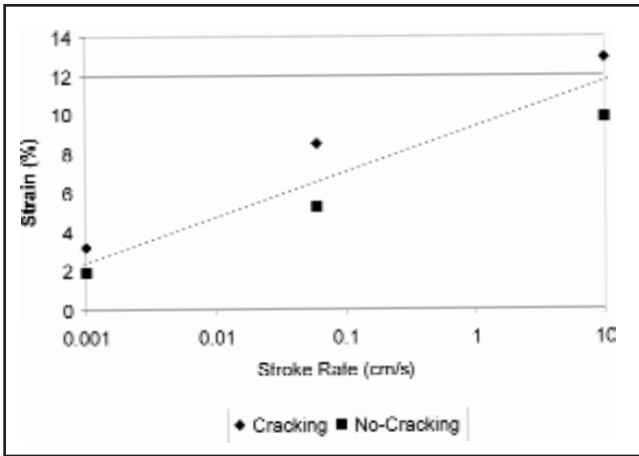


Fig. 9 — Effect of stroke rate on cracking threshold.

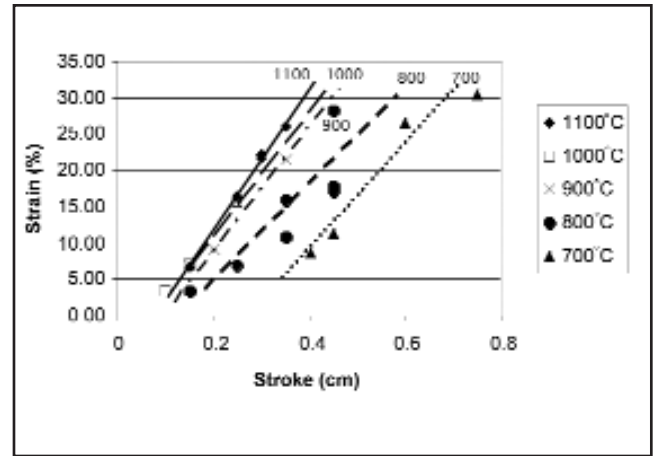


Fig. 10 — Stroke-to-strain relationship for Type 310 stainless steel at 0.06 cm/s at various temperatures.

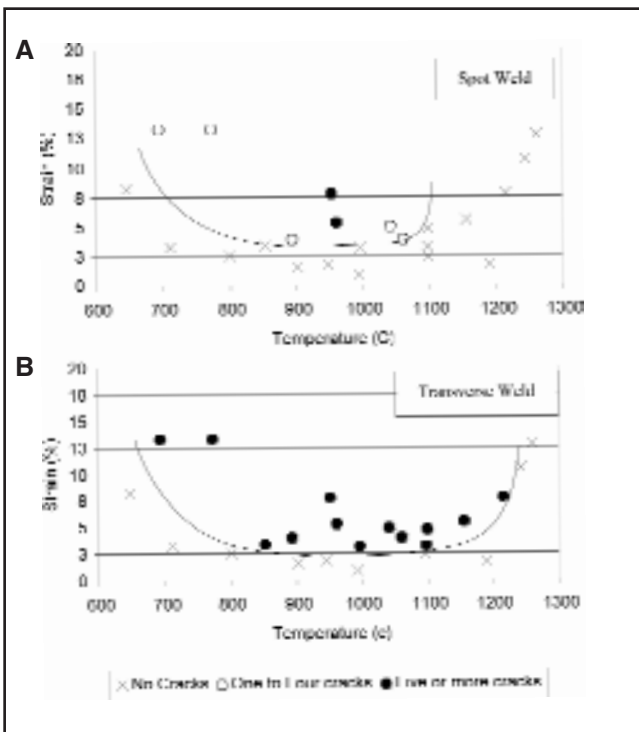


Fig. 11 — Comparison between: A — spot; and B — transverse prewelds in Alloy 690.

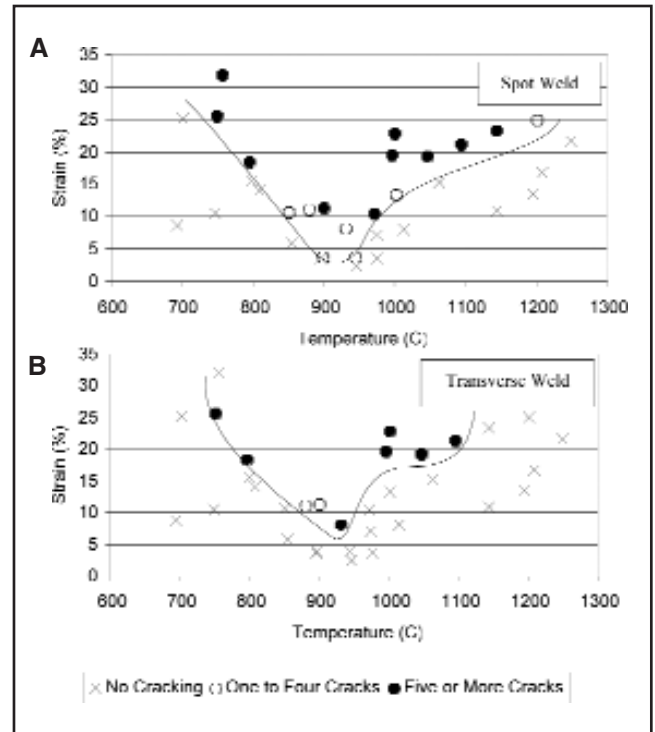


Fig. 12 — Comparison between: A — spot; and B — transverse prewelds in AL-6XN.

perature appeared to reduce susceptibility to DDC, thus it was decided to eliminate this step during standard testing until more extensive testing could be conducted.

Heating Rate to Test Temperature. To determine if the heating rate has any effect on the cracking threshold, two different heating rates were evaluated. The first of 100°C/s was chosen as an approximation of that encountered in GTA welding. The second of 10°C/s was selected to determine if the slower heating rate would have any effect. All of the other testing conditions

were set according to the standard conditions in Table 3. Results for the heating rate experiment are shown in Fig. 7.

With the given data, no significant variation in cracking threshold could be attributed to heating rate. As a result, 100°C/s was chosen as the standard heating rate for the remainder of the testing since it was more representative of actual welding conditions and minimized testing time.

Hold Time at Test Temperature. Hold time prior to application of stroke was also evaluated. For consistency, samples were

held at test temperature for an equal amount of time after the stroke was applied. A longer hold time gives the operator the opportunity to ensure that the temperature of the sample was precisely at the testing temperature and to adjust the stroke so that the load on the sample was approximately 0 prior to testing — Fig. 8. The different hold times were 1 s before stroke and 1 s after, 10 s before and 10 s after, and 300 s before and 300 s after. The remainder of the conditions were held constant according to Table 3. The results for the hold time at peak temperature are

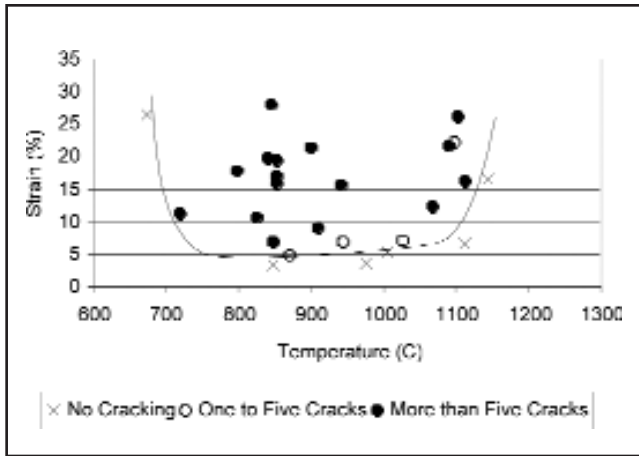


Fig. 13 — Temperature-strain envelope for Type 310 SS using standard conditions (sum of cracks from both transverse and spot prewelds).

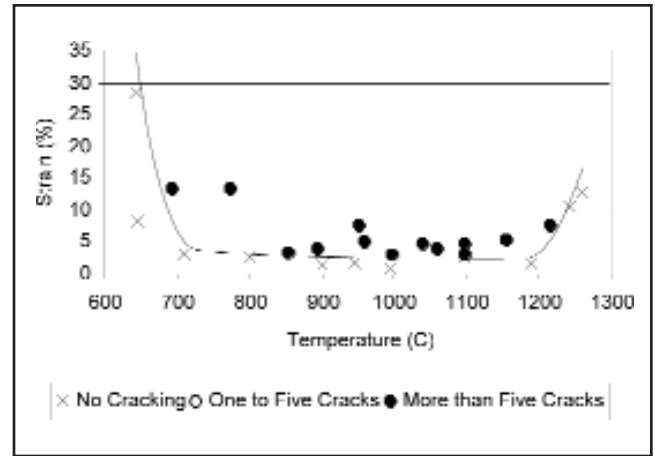


Fig. 14 — Temperature-strain envelope for Alloy 690 using standard conditions (sum of cracks from both transverse and spot prewelds).

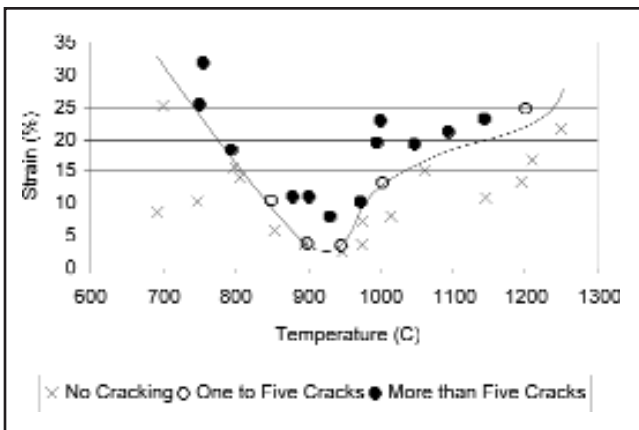


Fig. 15 — Temperature-strain envelope for AL-6XN using standard conditions (sum of cracks from both transverse and spot prewelds).

shown in Fig. 7.

Based on these results, no variation in cracking threshold can be determined from time at temperature within these ranges. Therefore, the setting of 10 s before and 10 s after was selected as it gave the operator sufficient time to make all necessary adjustments before the sample was strained without extending the length of the test.

Effect of Multiple Heating Cycles. There was some interest in the effect of multiple heating cycles to determine if it had any effect on test repeatability or DDC susceptibility in multi-thermal cycle welding procedures. Three different conditions were evaluated: 1, 3, and 11 heating cycles. A peak temperature of 1000°C and a rate of 100°C/s were used. In each case the stroke was applied at the peak temperature on the last heating cycle. Prior to the stroke application, adjustments were made to ensure the sample was not loaded as a result of thermal ex-

pansion and contraction. The results of the multiple heating cycle tests are displayed in Fig. 7.

The results indicate that there is no relationship between the number of thermal cycles and the threshold strain for cracking. Based on this, further testing was conducted using only a single thermal cycle.

Effect of Stroke

Rate. In response to the previously reported effects on cracking resulting from variation in stroke rate (Refs. 7, 15–17), three stroke rates were evaluated: 0.001, 0.06, and 10 cm/s. All of the other conditions were held constant according to Table 3. The results are shown in Fig. 9.

These results confirm that stroke rate does have an effect on the cracking threshold and that this is an important condition to consider when running the test. Using the condition established by Zhang et al. (Ref. 7) of 0.056 cm/s as being a good approximation with that of laboratory test welds, the stroke rate of 0.06 cm/s was chosen for these tests. Additional testing is required to determine the effect and importance of stroke rate.

Relationship between Stroke and Strain. The stroke-to-strain relationship varies as a function of temperature. Samples of Type 310 SS were run at a variety of temperature and stroke combinations to determine the relationship with strain. The results are displayed in Fig. 10. The data can be used as an approximation to

determine appropriate stroke levels for further testing. Similar data were not developed for Alloy 690 or AL-6XN.

Type of Preweld. For all of the materials tested, a spot preweld was placed on one side and a transverse preweld on the other — Fig. 4. After testing all three materials, a trend was noticed in the location of the cracks in the different materials. The cracking tended to occur preferentially in either the transverse or the spot weld, depending on the alloy in question. A comparison of the difference in prewelds for Alloy 690 is shown in Fig. 11 and for AL-6XN in Fig. 12. For Alloy 690, the cracking was more severe in the transverse prewelds than for the spot prewelds. However, for AL-6XN the cracking in the spot prewelds was more severe. Results for Type 310 stainless steel were mixed with the combination of both spot and transverse prewelds producing the most consistent results.

Final Procedure

Based on the preliminary testing, a set of final conditions was developed (Table 4) to test the three materials. The completed STF curves for Type 310, Alloy 690, and AL-6XN that were generated using these conditions are shown in Figs. 13, 14, and 15, respectively. For the final testing procedure, the sum of cracks in both the transverse and spot preweld was used as the result. For example, if there were two cracks in the spot weld and one in the transverse weld, the number of cracks reported would be three. Based on these, the ductility dip temperature range and the threshold strain (ϵ_{min}) were determined (Table 5). The DTR was determined at 15% strain for consistency among materials based on the recommendations of Zhang et al (Ref. 7).

Metallurgical Investigation

Metallographic samples were prepared for each material tested. While the samples all revealed migrated grain boundaries in the alloys tested (Figs. 16–18), Alloy 690 tended to have the straightest MGBs and was the most susceptible to cracking (Fig. 16). Precipitates and second phases tended to pin migrated grain boundaries in AL-6XN, causing tortuous boundaries that were more resistant to cracking — Fig. 17. At high temperature, evidence of recrystallization along the grain boundaries was observed (Fig. 19). The cracks tended to terminate at locations where the material started to recrystallize, indicating that the onset of recrystallization may determine the upper limit of the ductility dip, as previously reported (Refs. 1, 8, 16, 18).

Discussion

Development of the STF Test Procedures.

The STF test described here has proven successful in developing strain-temperature cracking envelopes that can be used to determine susceptibility to elevated temperature solid-state fracture. It should be recognized that the bulk of the procedure development was conducted using Type 310 stainless steel and that extensive evaluation of the effect of test parameters was not conducted on the other alloys. The following provides a summary and discussion of the test variables.

Test Temperature and Peak Temperature. Preliminary work has shown (Fig. 7) that peak temperature (on-heating vs. on-cooling test) does have an effect on cracking susceptibility. The literature (Refs. 5, 10, 19) would agree that there is some effect on peak temperature but is inconclusive as to what causes it. No recrystallization was observed in the sample heated to 1250°C and the grain size was comparable with samples tested at 1000°C. It is therefore likely that this phenomenon could be a segregation effect. It is also possible this variation could be caused by a difference between the on-cooling and on-heating ductility dip. Work by Nakagawa et al. (Ref. 19) found that the cracking occurred around the peak temperature of the first reheat, indicating the on-heating test for ductility dip may be more accurate. This condition is most closely repeated with the stroke applied during the on-heating portion. The peak temperature used should therefore be the same as the test temperature until more research can be conducted to understand the effects that peak temperature and other on-cooling conditions have on the test.

Heating Rate to Test Temperature. The

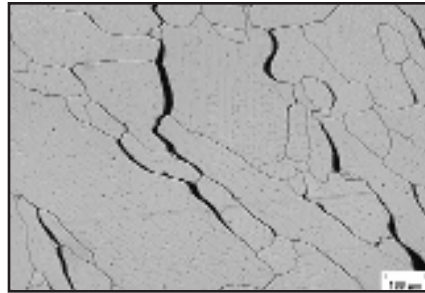


Fig. 16 — Ductile dip cracking in Alloy 690 tested at 951°C with preferred cracking along MGBs (10% chromic acid at 2.5 V).

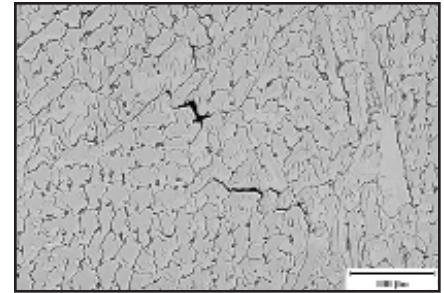


Fig. 17 — Ductile dip cracking in AL-6XN tested at 930°C showing tortuous migrated grain boundaries (10% oxalic acid at 2.5 V).

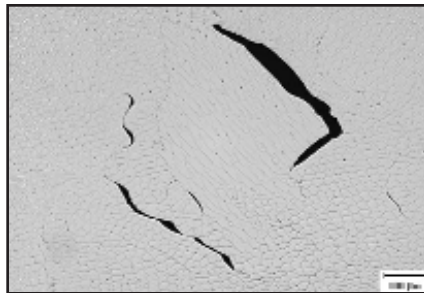


Fig. 18 — Ductile dip cracking in Type 310 stainless steel tested at 950°C with preferred cracking along MGBs (10% oxalic acid at 2.5 V).

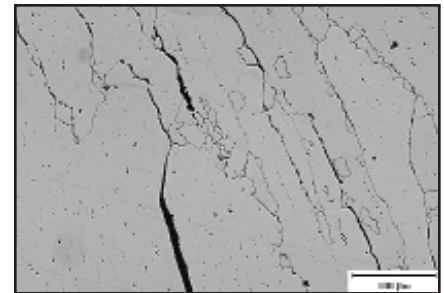


Fig. 19 — Ductile dip cracking in Alloy 690 tested at 1214°C. Note recrystallization at point (arrow) where the crack terminates MGBs (10% chromic acid at 2.5 V).

Table 4 — Standard STF Conditions

Parameters	Value
Constants	
Heating rate to test temperature	100°C/s
Hold time before stroke	10 s
Hold time after stroke	10 s
Number of heating cycles	1
Peak temperature	Same as test temperature
Type of preweld	Combined transverse and spot on each sample
Stroke rate	0.06 cm/s
Variables	
Test temperature	600 to 1300°C
Stroke length	0.05 to 0.75 cm

Table 5 — DTR (Temperature Range at 15% Strain) and Threshold Strain (ϵ_{min}) for Type 310, Alloy 690, and AL-6XN

Material	Ductility Dip Temperature Range (DTR)	Threshold Strain (ϵ_{min})
Type 310 stainless steel	675 to 1125°C	4%
Alloy 690	650 to 1250°C	2.5%
AL-6XN	800 to 1050°C	3%

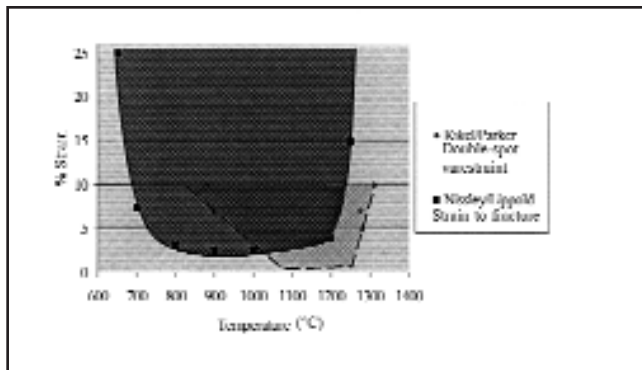


Fig. 20 — Comparison of DDC results between double-spot varestraint (Ref. 13) and strain-to-fracture for Alloy 690.

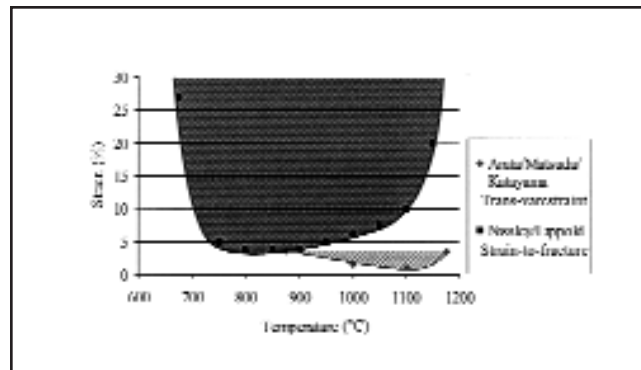


Fig. 21 — Comparison between trans-varestraint (Ref. 6) and strain-to-fracture for Type 310 stainless steel.

heating rate of 100°C/s was selected initially as a reasonable approximation of the heating rate observed in GTA welds. No microstructural difference was observed between samples heated at 10 and 100°C/s. In the literature, Zhang et al. (Ref. 7) used a heating time of 9 s to peak temperature for a variety of DDC temperatures (500–1200°C), with resulting heating rates ranging from 56 to 133°C/s. As anticipated, the time at temperature that samples were exposed to during heating was insufficient to cause variation in grain growth or precipitation formation and growth. As a result of this, the use of 100°C/s heating rate was selected as a reasonable approximation of actual weld heating rates, as no significance could be attributed to the effect of heating rate for Type 310 — Fig. 7. The effect of heating rate should be reevaluated for body-centered cubic (BCC) materials where diffusion rates are higher than those in FCC materials.

Hold Time at Test Temperature. Hold time is a significant test variable as it allows the user time to trim the temperature and to adjust the stroke to account for any thermal expansion in the sample. If the hold time had a considerable effect on cracking threshold, a delay time of zero would be required for consistency. Yenisavich (Ref. 15) reported that the on-heating ductility was almost the same with and without a delay (hold time). However, he reported great differences between the on-cooling curves with and without a 10-s delay (hold). Testing done for this project was conducted only on the on-heating portion of the ductility curve. The results of Type 310 (Fig. 7) showed no variation in cracking attributed to hold time, which agreed with Yenisavich. Similar to heating rate, the microstructures of the samples did not vary significantly among the different times. Again, the time at temperature was not sufficient to promote extensive grain growth, which could have affected the cracking susceptibility. Due to

this, a hold time of 10 s before stroking was used because it allowed sufficient time for adjustments of on-heating tests. Future work will have to address on-cooling effects if this test is to be used for the on-cooling portion of the curve.

Number of Heating Cycles. The number of heating cycles is an important and practical factor for testing. It was examined to determine if there were any observed beneficial or detrimental effects caused by multiple heating cycles. During normal multipass welding procedures, the sample would only be heated into the DDC temperature range during several subsequent passes, depending on geometry and welding conditions. While multipass welds are susceptible to DDC, it was unclear if the thermal history of the sample alone had an effect on cracking or if other conditions such as microstructure, accumulated stress in the system, or a combination of these had an effect on cracking.

Results in Fig. 7 show no major effect from multiple heating cycles, which would indicate that a sample heated to temperature but not tested can still be used to obtain valid results. Evaluation of the microstructures resulted in no significant variation between samples with different numbers of heating cycles. As with heating rate and time at temperature, the number of heating cycles does not affect cracking susceptibility because it is not at elevated temperature for long enough to sufficiently affect the microstructure (grain size and precipitation).

Stroke Rate. The stroke rate used when evaluating a material has been shown here to be important, as was reported in the literature (Refs. 7, 15–17). Results obtained with the STF test showed that the cracking severity decreased with increasing stroke rate, which agrees with the literature. The stroke rate of 0.06 cm/s was selected based upon the recommended value of 0.056 cm/s by Zhang et al. (Ref. 7), which they found to have good

correlation when used with their Gleeble hot ductility test and the crack susceptibility obtained in their weld cracking test. The material they tested was Fe-36%Ni (Invar), and a direct comparison with their results is not possible because of the different materials tested here.

Samples run at different stroke rates were microstructurally similar and no change in cracking susceptibility could be attributed to the microstructure. This variation in cracking from stroke rate may be the result of a time factor in the mechanism for DDC. At slower stroke rates (longer time) the preferred mechanism for stress relaxation may be DDC, while at higher stroke rates (short time) another mechanism may occur preferentially, such as intragranular plastic deformation, before sufficient time passes for the mechanism for DDC to occur. Until other information indicates otherwise, the stroke rate of 0.06 cm/s should be used for comparison purposes among different materials.

Type of Preweld. The use of a preweld was driven by the desire to produce “fresh” weld metal that is not affected by multiple welding cycles and therefore has a known thermal history. This approach is better than cutting samples from multipass welds where thermal history is unknown and not reproducible from sample to sample. In addition, in the case of the spot weld, current ramping was used while making prewelds to produce large epitaxial grains growing to the center of the spot and to avoid crater cracking.

There were several tests that used prewelds that are documented. They included spot (Ref. 13), transverse (Ref. 7), and longitudinal welds (Ref. 12). However, little is mentioned regarding the use of different prewelds or of any advantage of a variety of prewelds. The choice of appropriate preweld for the STF test was not a simple choice. While a transverse or longitudinal weld most accurately represents the type of weld used most often in appli-

cations where DDC is a problem, the spot weld produced a favorable microstructure that has grains oriented in all directions to the applied load. Initially a test matrix was constructed to compare transverse, longitudinal, and spot prewelds in the STF test. Early results indicated cracking occurred primarily in transverse and spot welds and was not as reproducible in longitudinal welds. The grain orientation relative to the strain in the longitudinal welds was not the same as that found in the spot and transverse, accounting for the difference in cracking. Evaluation of the sample with both transverse and spot prewelds produced differing results. In some materials the transverse weld produced more cracks (Fig. 11), while in another, the spot weld was more susceptible (Fig. 12). It is possible that for the transverse prewelds, the solidification differences (teardrop vs. elliptical) between materials could have caused variation in grain orientation, resulting in cracking variation. It was concluded that for the remainder of this work, the results of both types of prewelds would be combined and reported as one, as it provided the most conservative results. However, from a theoretical understanding, the spot preweld should provide more consistent results because it produces grain boundaries in a range of orientations from the center and is, therefore, not dependent on the direction of the applied load. The authors recommend that for future work the spot preweld be used on either one or both sides of the samples. Spot prewelds on both sides could be used to increase the sensitivity to cracking (by increasing the weld area and number of grain boundaries). This could also be used in cases where multiple conditions are to be tested with one sample, where each preweld is made under different conditions (shielding gas, impurity addition, etc.). Since this initial work, additional testing has been done successfully with the use of spot welds only (Refs. 20, 21).

Comparison with Other DDC Results

Alloy 690. Alloy 690 was reported susceptible to DDC by Kikel and Parker (Ref. 13) and results of the double-spot (spot-on-spot) vareststraint and spot vareststraint were reported. The samples were tested at 5-, 7-, and 10%-augmented strain with a constant bend rate of 25.4 cm/s. A comparison of their results with the STF data (Fig. 14) is shown in Fig. 20. The strain-to-fracture results were tested over a range of strains from 2 to 25% at a strain rate of 0.06 cm/s. The results of the double-spot vareststraint test are shifted approximately 75–150°C to higher temperatures relative to the STF results. This may have been caused by the difference in stroke rate

(Fig. 9), material composition variations, or the smaller DDC susceptible region found in vareststraint testing as a result of the steep temperature gradient.

While the threshold strain for the vareststraint test was reported as 1%, no testing was actually conducted below 5% in the double-spot vareststraint test. This limits the use of the vareststraint for accurately determining threshold strain. For this case, the strain-to-fracture test appears to be a more sensitive method for developing a ductility dip curve than that of the double-spot vareststraint test.

Type 310 Stainless Steel. Research by Arata et al. (Ref. 6) included results on DDC susceptibility in Type 310S stainless steel. The results were obtained with the trans-vareststraint test with 1–3.75% augmented strain with the stroke applied almost instantly (60%/s). A comparison of these results along with those produced using the strain-to-fracture test (Fig. 13) are shown in Fig. 21. The strain-to-fracture test was performed from 3 to 27% strain at 0.06 cm/s. The upper temperatures did not differ significantly but the lower temperatures differed by approximately 200°C. Similar to the previous discussion, this variation may be the result of the difference in stroke rate (Fig. 9), material composition variations, or the smaller DDC susceptible region found in vareststraint testing as a result of the steep temperature gradient. The threshold strain is very different in the two cases and it is not clear what the cause of the variation is. It is possible that the two heats of Type 310 used had different susceptibilities to DDC because of variations in composition (significant Si content difference). The transverse vareststraint (Ref. 6) evaluates cracking in the primary weld bead as it was cooling, which is reported (by Yenicavich [Ref. 15]) to be lower, while the STF test evaluated the weld metal during a subsequent reheat.

Test Benefits

Most of the initial problems associated with the other testing methods have been addressed by the Gleeble-based STF test. Most importantly, because of temperature control, solidification and liquation cracks are not present in the samples. The area of the sample heated to the test temperature is relatively large and has a shallow thermal gradient in the center. Both the temperature control and thermal gradient make evaluation of DDC in a sample easier. The absence of other types of cracks ensures nothing else is affecting the measurement of strain in the sample. The use of ramping current control for the pre-spot has eliminated crater cracks in the spot welds and has produced large

epitaxial grains growing to the center of the spot. The STF test allows samples to be evaluated on all sides because the strain is applied along the axis of the sample and there is no maximum strain level. This has been beneficial in determining the cracking threshold of materials and for determining the ductility dip characteristics above 10% (limit of the vareststraint). In addition, the vareststraint is limited to testing in strain increments (1, 2, 3,...) while the STF is continuous and thus is not limited.

The sample design for the strain-to-fracture is relatively simple and can be made out of standard plate material and with the use of GTAW equipment. Samples can be made with a variety of prewelds to accommodate different testing variables. Testing variables can be easily isolated to determine single effects or varied as in a statistical DOE (design of experiments) approach. Data from the STF test are not dependent upon the operators' ability to obtain the exact testing temperature or strain, because the testing temperature acquired from the data acquisition and actual strain are what is reported. This negates small differences in the way the test is run for multiple operators or different thermomechanical simulators. This test has proven itself as a robust and reproducible test for quantifying DDC susceptibility in austenitic materials.

Collins (Refs. 20, 21) has also tested DDC susceptibility in filler metal deposits using the STF test. Samples were cut out of all, weld, metal test plates and a spot preweld was performed on the samples. Using the same conditions as developed in this work (Table 4), temperature-strain envelopes have been developed for different Ni-based filler metal compositions.

Insight into Mechanism

While the mechanism for DDC is still not fully understood, the STF test has confirmed many previous theories about DDC and has proven itself as a valuable method to test different conditions and produce a variety of cracked samples for evaluation. Results from this research confirm that DDC occurs preferentially along migrated weld metal grain boundaries (Fig. 16), as is generally accepted (Ref. 8). Weld metal was found more susceptible to cracking than wrought base metal, which exhibited no cracking in these tests. Weld metals with precipitates or second phases tend to restrict grain boundary motion and thereby reduce the amount and length of cracking, as was observed in the case of AL-6XN (Fig. 17). The susceptibility to cracking is dependent upon temperature, strain, and stroke rate (not exclusively). The cracks occurred

in the sample when strain achieved a threshold level indicating that DDC is a mechanism connected with deformation. Recrystallization was observed at the upper temperatures of the DDC range (Fig. 19), agreeing with the literature (Refs. 1, 8, 16, 18) that recrystallization results in the recovery of ductility at higher temperatures. The relationship between DDC and stroke rate (Fig. 9) indicates there are competing deformation mechanisms and time is a factor in determining which mechanism dominates. The limiting factor for DDC could be associated with the time for grain boundary sliding to occur. Much work is still required to develop a full understanding of the mechanism for DDC.

Conclusions

1) The strain-to-fracture test (STF) is an effective method for producing ductility dip cracks and quantifying susceptibility to elevated temperature, solid-state cracking.

- Temperature and strain control are better than with other tests (such as the vareststraint).
- Sample preparation is easy and inexpensive.
- Evaluation of cracking is more straightforward.

2) STF test procedures have been developed based on evaluation of a variety of test variables. This test procedure should be applicable to most austenitic materials. The following conclusions can be made about the test variables.

- Stroke rates ranging from 0.001 to 10 cm/s affected the ductility dip temperature range (DTR) and the threshold strain for cracking (ϵ_{min}). Higher stroke rates caused a decrease in the DTR and an increase in the ϵ_{min} .
- Hold time at peak temperature from 1 to 300 s did not have an effect on DDC cracking susceptibility.
- Multiple heating cycles alone, ranging from 1 to 11 cycles, did not have an effect on DDC cracking susceptibility.
- Different STF results are obtained with on-cooling tests as compared to on-heating tests. For example, heating to 1250°C prior to testing to 1000°C increased the critical STF.
- Heating rate to peak temperature of 10 and 100°C/s did not have an effect on DDC cracking susceptibility.
- Prewelds were effective in producing a microstructure susceptible to DDC. A combination of a transverse and a spot preweld on each sample produced the most consistent results.

3) Metallurgical.

- Cracking occurred along crystallographic grain boundaries generally referred to as migrated grain boundaries (MGBs) in austenitic weld metal.
- Materials with few precipitates or second phases had the straightest MGBs and exhibited greater susceptibility to DDC than those with tortuous grain boundaries.
- Recrystallization was observed at the upper temperatures of the DTR and coincided with the recovery of ductility.

4) Comparison with other work.

- DDC results of the STF test reasonably compared with those previously reported using the vareststraint test.
- Results of the vareststraint are shifted to higher temperatures when compared with the STF test. This may be due to errors in temperature measurement in the vareststraint or differences in strain rates.

5) The DDC susceptibility of the materials tested, reported from highest to lowest, is as follows:

- Alloy 690 (DTR 650 to 1250°C, ϵ_{min} 2.5%).
- Type 310 stainless steel (DTR 675 to 1125°C, ϵ_{min} 4%).
- AL-6XN (DTR 800 to 1050°C, ϵ_{min} 3%).

Acknowledgments

This project was supported by a fellowship provided by the American Welding Society Foundation. The authors are very grateful for its support of this project and its commitment to higher education. The authors would also like to thank BWXT Inc. for providing the Alloy 690 material.

References

1. Rhines, F. N., and Wray, P. J. 1961. Investigation of the intermediate temperature ductility minimum in metals. *Transactions of the ASM* 54: 117-128.
2. Hemsworth, B., Boniszewski, T., and Eaton, N. F. 1969. Classification and definition of high temperature welding cracks in alloys. *Metal Construction and British Welding Journal* (2): 5-16.
3. Nissley, N. 2002. Development of the strain-to-fracture test to study ductility-dip cracking in austenitic alloys. M.S. thesis, Ohio State University, Columbus, Ohio.
4. Nissley, N. E., and Lippold, J. C. 2002. Development of a test technique for evaluating ductility-dip cracking susceptibility in austenitic alloys. *ASM 6th International Conference on Trends in Welding Research*. Pine Mountain, Ga. April 2002.

5. Hadrill, D. M., and Baker, R. G. 1965. Microcracking in austenitic weld metal. *British Welding Journal* 12 (9).
6. Arata, Y., Matsuda, F., and Katayama, S. 1977. Solidification crack susceptibility in weld metals of fully austenitic stainless steels (Report II). *Transactions of JWRI*, 6/1 (6): 105-116.
7. Zhang, Y. C., Nakagawa, H., and Matsuda, F. 1985. Weldability of Fe-36%Ni alloy (Report III). *Transactions of JWRI* 14/1 (7): 107-114.
8. Lippold, J. C., Rowe, M. D., and Juhas, M. C. 1997. Summary of ductility dip cracking. Unpublished work at Ohio State University, Columbus, Ohio.
9. Lippold, J. C., Clark, W. A. T., and Tumuru, M. 1992. An investigation of weld metal interfaces. *The Metal Science of Joining*. Warrendale, Pa.: The Metals, Minerals and Materials Society, pp. 141-146.
10. Yeniscavich, W. 1970. Correlation of hot ductility curves with cracking during welding. *Methods of High-Alloy Weldability Evaluation*. Philadelphia, Pa.: Welding Research Council, pp. 2-12.
11. Honeycombe, J., and Gooch, T. G. 1970. Microcracking in fully austenitic stainless steel weld metal. *Metal Construction and British Welding Journal* 2(9): 375-380.
12. Nishimoto, K., Mori, H., Esaki, K., Hongoh, S., and Shirai, M. *Effect of Sulfur and Thermal Cycles on Reheat Cracking Susceptibility in Multi-pass Weld Metal of Fe-36%Ni Alloy*. IIW Doc. IX-1934-99.
13. Kikel, J. M., and Parker, D. M. 1998. Ductility dip cracking susceptibility of Filler Metal 52 and Alloy 690. *Trends in Welding Research*. Pine Mountain, Ga., June 1 - 5, pp. 757-762.
14. Unpublished work at EWI, September 1997.
15. Yeniscavich, W. 1966. A correlation of Ni-Cr-Fe alloy weld metal fissuring with hot ductility behavior. *Welding Journal* 45(8): 344-s to 355-s.
16. Zhang, Y. C., Nakagawa, H., and Matsuda, F. 1985. Weldability of Fe-36%Ni alloy (Report V). *Transactions of JWRI* 14/2(12): 119-124.
17. Mintz, B. Abu-Shosha, R., and Shaker, M. 1993. Influence of deformation induced ferrite, grain boundary sliding, and dynamic recrystallisation on hot ductility of 0.1-0.75%C steels. *Materials Science and Technology* 9 (10): 907-914.
18. Zhang, Y. C., Nakagawa, H., and Matsuda, F. 1985. Weldability of Fe-36%Ni alloy (Report VI). *Transactions of JWRI* 14/5(12): 125-134.
19. Nakagawa, H., Matsuda, F., Nagai, A., and Sakabata, N. 1980. Weldability of Fe-36% Ni alloy (Report 1) — Hot cracking with cross-bead test. *Transactions of JWRI* 9/2(12): 55-62.
20. Collins, M. 2002. An investigation of ductility dip cracking in nickel-base filler materials. M.S. thesis, Ohio State University, Columbus, Ohio.
21. Collins, M. G., and Lippold, J. C. 2002. Ductility-dip cracking mechanism development in austenitic, nickel-base weld metals. *ASM 6th International Conference on Trends in Welding Research*. Pine Mountain, Ga., April 2002.